

1 Simulation

This chapter is dedicated to a simulation study that illustrates the finite-sample behavior of the LIVE estimators $\hat{v}_\alpha(y_\alpha)$ and $\hat{v}_{\alpha\beta}(y_\alpha, y_\beta)$. For simplicity, we consider examples with zero conditional mean function only.

Example 1 *We define the process*

$$y_t = \sqrt{4 + v_1(y_{t-1}) + v_2(y_{t-2}) + v_3(y_{t-3}) + v_{12}(y_{t-1}, y_{t-2}) + v_{13}(y_{t-1}, y_{t-3}) + v_{23}(y_{t-2}, y_{t-3})} \varepsilon_t$$

where $v_1(u) = v_2(u) = -v_3(u) = 0.5\sin(u)$,

$v_{12}(u, v) = v_{13}(u, v) = v_{23}(u, v) = 0.5\arctan(u)\arctan(v)$, ε_t independent of \mathcal{F}_{t-1} and $\varepsilon_t \sim \text{Uniform}(-\sqrt{3}, \sqrt{3})$.

The components of the volatility function are selected to satisfy conditions of Lu and Jiang (2001) to ensure the geometric ergodicity (and, therefore, the strict stationarity) of the process y_t . Condition (B1) of Lu and Jiang (2001) reduces in the one-dimensional case to the requirement that the growth rate in each coordinate must not exceed the linear one; apparently, the product of arctan functions satisfies this condition. Based on this model, we simulate 500 samples with sample size $n = 500$. For each realization of the ARCH process, we apply the instrumental variable estimation procedure from Section 3.2 to obtain estimates of $v_\alpha(\cdot)$ and $v_{\alpha\beta}(\cdot)$, $1 \leq \alpha, \beta \leq 3$. Gaussian kernels (univariate or product multivariate as needed) are used for all of the nonparametric estimates. Bandwidth g is selected according to the Gaussian rule of thumb as $g = cn^{-1/(l+4)}$ where $c = (\frac{4}{l+2})^{1/(l+4)}$ and l is the number of dimensions of the function to be estimated. For example, $l = 1$ for any one-dimensional marginal density, $l = 2$ for $\hat{p}_{\alpha\beta}(y_\alpha, y_\beta)$, $l = d$ for $\hat{p}(\mathbf{y})$, etc. (see, for example, Wand and Jones (1995) for details). The constant c is selected to ensure that the bandwidth g is asymptotically optimal in the mean squared error sense under the assumption that the true density is Gaussian. The same rule is used to select the second bandwidth h where $l = 1$ or $l = 2$ for additive and interactive components, respectively. To evaluate the performance of the estimators, the mean squared error (MSE) and the mean absolute deviation error (MAE) are computed for each simulated sample. They are

Table 1: AVERAGED MSE AND MAE FOR SIX VOLATILITY ESTIMATORS IN THE UNIFORM DISTRIBUTION CASE

	v_1	v_2	v_3	v_{12}	v_{13}	v_{23}
MSE	0.33	0.31	0.30	0.54	0.56	0.53
MAE	0.25	0.24	0.24	0.36	0.37	0.36

defined as

$$\begin{aligned}
MSE(v_\alpha) &= \left\{ \frac{1}{101} \sum_{j=1}^{101} [v_\alpha(x_j) - \hat{v}_\alpha(x_j)]^2 \right\}^{1/2}, \\
MSE(v_{\alpha\beta}) &= \left\{ \frac{1}{2601} \sum_{j=1}^{2601} [v_{\alpha\beta}(x_{j,1}, x_{j,2}) - \hat{v}_{\alpha\beta}(x_{j,1}, x_{j,2})]^2 \right\}^{1/2}, \\
MAE(v_\alpha) &= \frac{1}{101} \sum_{j=1}^{101} |v_\alpha(x_j) - \hat{v}_\alpha(x_j)|, \\
MAE(v_{\alpha\beta}) &= \frac{1}{2601} \sum_{j=1}^{2601} |v_{\alpha\beta}(x_{j,1}, x_{j,2}) - \hat{v}_{\alpha\beta}(x_{j,1}, x_{j,2})|,
\end{aligned}$$

$1 \leq \alpha < \beta \leq 3$. In the above, $\{x_j\}_{j=1}^{101}$ is an equispaced grid on $[-4, 4]$, and $\{x_{j,1}\}_{j=1}^{51} \times \{x_{j,2}\}_{j=1}^{51}$ is an equispaced grid on $[-4, 4] \times [-4, 4]$. The grid range covers more than 99% of all observations in both one- and two- dimensions so very little information is lost. Table (1) shows averages of MSE's and MAE's for all six components from 500 repetitions. Figure (1) shows the averaged estimates of three additive components as well as the true functions; the solid lines in red are the true curves and the dotted ones in black are the estimates averaged over 500 repetitions. Figures (2) through (5) show the true surface of the interactive components next to the estimates averaged over 500 simulations. In general, the results show a very good fit for both additive and interactive components; among interactive components, $v_{12}(\cdot)$ and $v_{23}(\cdot)$ seem to have been fit particularly well. It can be clearly seen that the use of local polynomial regression eliminated boundary effects to a great extent in both additive and interactive component estimation.

Example 2 *Again, consider the model*

$$y_t = \sqrt{4 + v_1(y_{t-1}) + v_2(y_{t-2}) + v_3(y_{t-3}) + v_{12}(y_{t-1}, y_{t-2}) + v_{13}(y_{t-1}, y_{t-3}) + v_{23}(y_{t-2}, y_{t-3})} \varepsilon_t$$

where

$$v_1(u) = v_2(u) = -v_3(u) = 0.5 \sin(u)$$

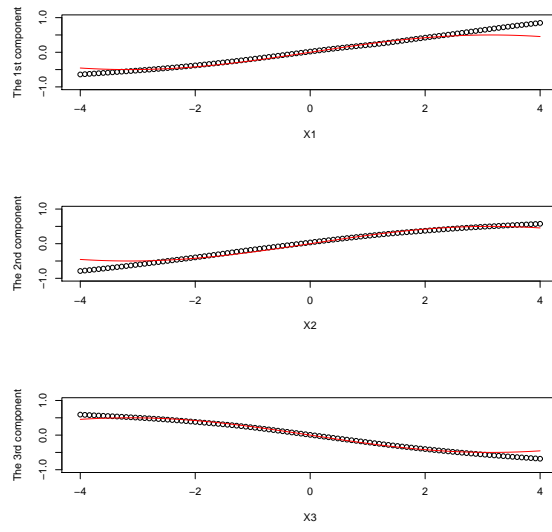


Figure 1: Estimates of three additive components in example 1

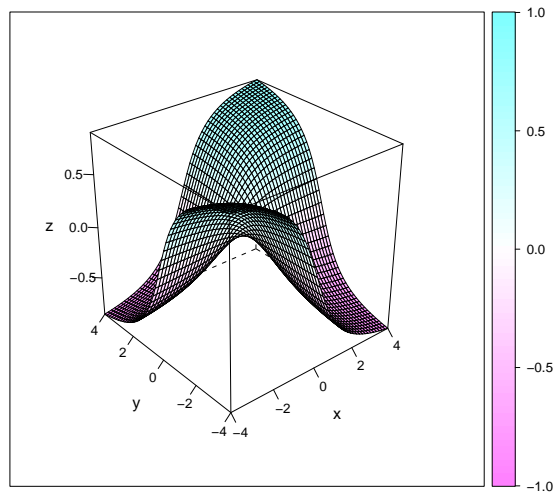


Figure 2: True surface of the interactive components in example 1

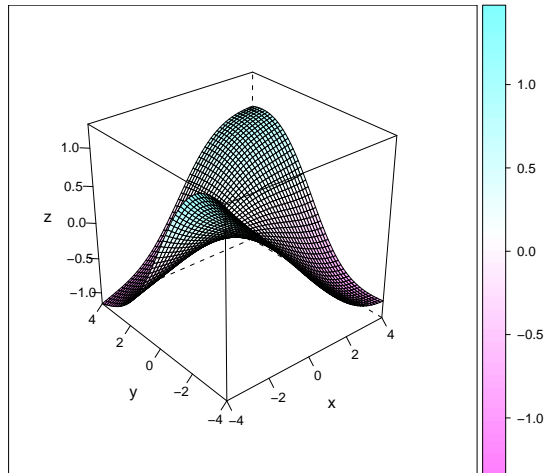


Figure 3: Estimated surface of $v_{12}(\cdot)$ in example 1

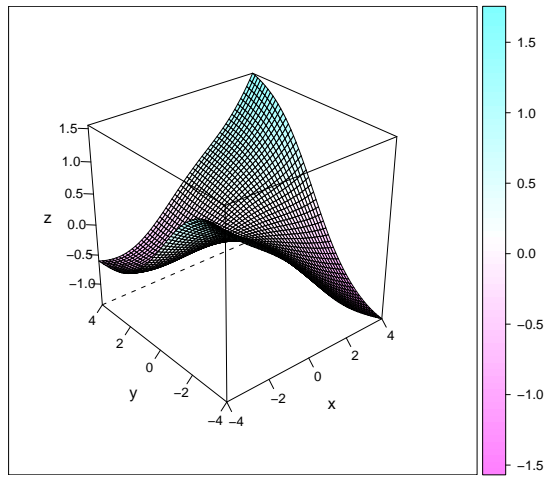


Figure 4: Estimated surface of $v_{13}(\cdot)$ in example 1

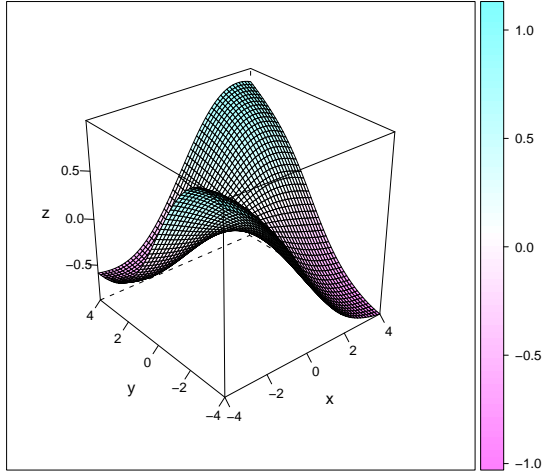


Figure 5: Estimated surface of $v_{23}(\cdot)$ in example 1

$$v_{12}(u, v) = v_{13}(u, v) = v_{23}(u, v) = 0.5 \arctan(u) \arctan(v)$$

ε_t independent of \mathcal{F}_{t-1} and $\varepsilon_t \sim N(0, 1)$

The previous example has the finitely supported error(innovation) distribution and this may not be realistic enough in practice. Therefore, we are interested in testing the performance of the method in case where the innovation distribution does not have a compact support. Obviously, the most intuitive choice is the standard normal distribution. The grid ranges we chose are $[-3.2, 3.2]$ in one-dimensional regressions and $[-3.2, 3.2] \times [-3.2, 3.2]$ in two-dimensional ones. These ranges cover approximately 90% and 80% of all observations, respectively. The averages of MSE's and MAE's for all the six components from 500 repetitions are shown in table (2). Note that the performance of the method does not seem to be any worse compared to the previous example. While additive components seem to be estimated with slightly less precision, the opposite is true when it comes to interactive components for either choice of the loss function. The averaged estimates of six volatility components as well as the true ones are presented in figures (6) through (10).

Table 2: AVERAGED MSE AND MAE FOR SIX VOLATILITY ESTIMATORS IN THE NORMAL DISTRIBUTION CASE

	v_1	v_2	v_3	v_{12}	v_{13}	v_{23}
MSE	0.40	0.40	0.39	0.41	0.40	0.42
MAE	0.32	0.32	0.32	0.31	0.30	0.31

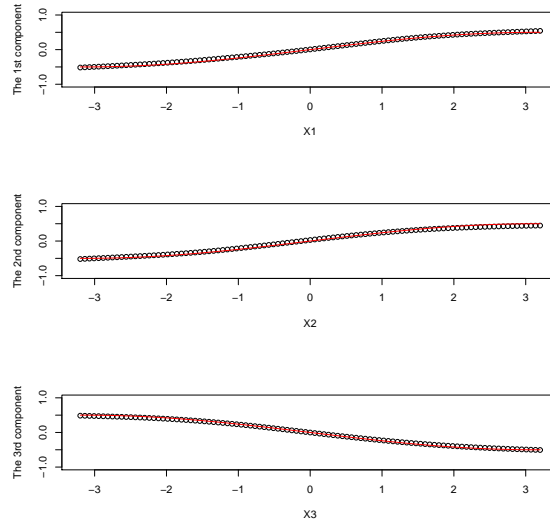


Figure 6: Estimates of three additive components in example 2

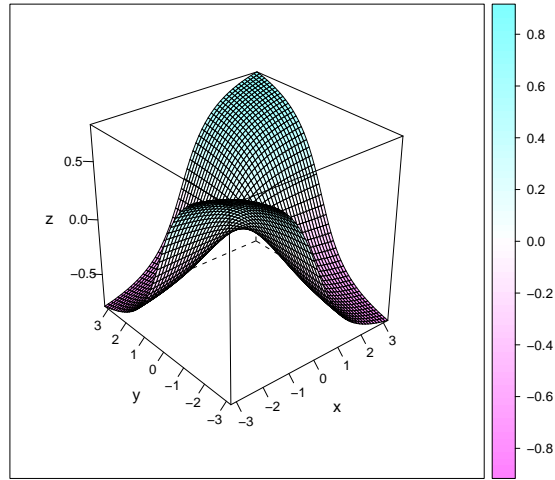


Figure 7: True surface of the interactive components in example 2

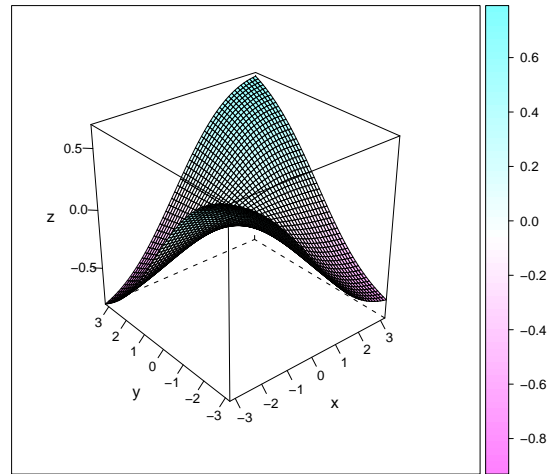


Figure 8: Estimated surface of $v_{12}(\cdot)$ in example 2

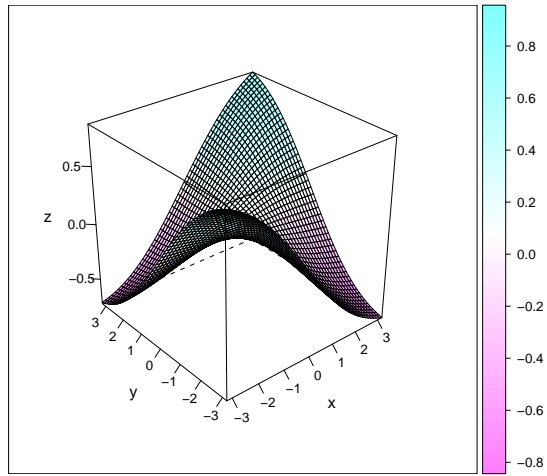


Figure 9: Estimated surface of $v_{13}(\cdot)$ in example 2

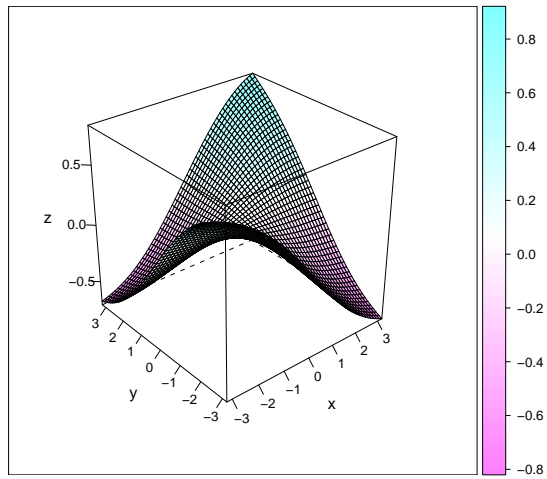


Figure 10: Estimated surface of $v_{23}(\cdot)$ in example 2